Supplementary material to

Flow induces blood-brain barrier and glycocalyx-related genes and negative surface charge in a lab-on-a-chip human culture model

Ana R. Santa-Maria[1,2,3], Fruzsina R. Walter[1,3], Ricardo Figueiredo[4,5], András Kincses[1,6], Judith Vigh[1,2], Marjolein Heymans[7], Maxime Culot[7], Peter Winter[4], Fabien Gosselet[7], András Dér[1], Maria A. Deli[1, *]

[1] Institute of Biophysics, Biological Research Centre, Temesvári krt. 62, H-6726, Szeged, Hungary

[2] Doctoral School of Biology, University of Szeged, Közép fasor 52, H-6726, Szeged, Hungary

[3] Department of Biotechnology, University of Szeged, Közép fasor 52., H-6726, Szeged, Hungary

[4] GenXPro GmbH, Altenhöferallee 3, D-60438, Frankfurt-Am-Main, Germany

[5] Johann Wolfgang Goethe University Frankfurt, Frankfurt-Am-Main, Germany

[6] Doctoral School of Multidisciplinary Medical Sciences, University of Szeged, Tisza Lajos körút 109., H-6725, Szeged, Hungary

[7] Univ. Artois, UR 2465, Laboratoire de la Barrière Hémato-Encéphalique (LBHE), F-62300 Lens, France

* Corresponding author:
Mária A. Deli,
Institute of Biophysics, Biological Research Centre, Temesvári krt 62, H-6726, Szeged, Hungary
Tel. +36-62-599602
e-mail: deli.maria@brc.hu

Methods

LOC device

The device was built as described in our previous publication.[5] Briefly, the top and bottom channels were fabricated from poly(dimethylsiloxane) (PDMS, Sylgard 184, Dow Corning GmbH, Wiesbaden, Germany), separated by a porous membrane (PET, 0.45 μm pore size, $2 \times 10^6/cm^2$ pore density and 23 μm thickness; It4ip, Louvain-la-Neuve, Belgium) (Figure 1(a)). The length, width and height of the top and bottom channels were 36 mm×2 mm×1 mm and 57mm×2 mm×2 mm, respectively. Gold electrodes (thickness: 25 nm) were formed on the plastic microscope slides using sputter-coating, providing low resistance to allow transendothelial electrical resistance (TEER) measurements and good visibility to monitor cell growth by phase contrast microscopy throughout the whole length of the channel.[5] The electrodes were linked connected with copper wires to a 4-channel voltohmmeter (EVOM^2; World Precision Instruments Inc., Sarasota, FL, USA). The PDMS channels were sandwiched between the plastic slides, and closed with plastic screws (Figure 1(a)). The device was sterilized with oxygen plasma for 5 min and 70% ethanol for 30 min before cells were seeded to the system.

Cell culture of the human endothelial cells and bovine pericytes

The in vitro BBB model, consisting of human endothelial cells in co-culture with bovine brain pericytes, was described by Cecchelli et al., 2014 and is named brain-like endothelial cells (BLECs). The isolation of $CD34^+$ cells required the collection of human umbilical cord blood from infants, which was approved by the Hospital ethical committee (Béthune Maternity Hospital, Béthune, France). Infants' parents signed an informed consent form, in compliance with the French legislation. The protocol was approved by the French Ministry of Higher Education and Research (CODECOH Number DC2011-1321). All experiments were carried out in accordance with the approved protocol and the World Medical Association Declaration of Helsinki. Briefly, the hematopoietic stem cells were isolated from human cord blood and differentiated to endothelial cells as previously published (Pedroso et al., 2011). These human endothelial cells (hEC) were seeded in 0.2% gelatin (type A from porcine skin) coated culture dishes and kept in endothelial cell culture medium (ECM, Sciencell, Carlsbad, CA, USA) supplemented with 5 % fetal bovine serum (FBS, heat inactivated), 1 % endothelial cell growth supplement (ECGS, Sciencell), and gentamycin (50 μg/ml). After reaching confluency, usually 2 days after seeding, hECs were gently trypsinized and 80×10^3 cells seeded into the porous polyester membrane of the lab-on-a-chip (LOC) device (Figure 1(b)). The membrane was coated with Matrigel (growth factor reduced BD Matrigel Matrix, BD Biosciences, Franklin Lakes, NJ, USA) at a dilution of 1:48.

Bovine brain pericytes (PCs) were isolated from brain microvessels as described earlier (Cecchelli et al., 2014). Permission for the protocol was obtained from the Ethical Committee of the University of Artois. Experiments were made according to "Guidance on good cell culture practice. A report of the second ECVAM task force on good cell culture practice" (Coecke et al., 2005). PCs were cultured in 0.2% gelatin coated dishes

in Dulbecco's modified Eagle's medium (DMEM, Life Technologies, Thermo Fisher Scientific, Waltham, MA, USA) supplemented with 20% FBS, 1% Glutamax (Life Technologies) and gentamicin (50 µg/ml). Cells were kept in culture until reaching confluency. Then, PCs were trypsinized and 25×10^3 cells were added to the bottom compartment of the LOC device, which was coated with 0.2% gelatin. The co-culture started when PCs were added (Figure 1(b)). During co-culture both compartments received hEC medium. The LOC device with the cells was kept at 37°C in a humified atmosphere and 5% CO_2.

The human *in vitro* BBB model used for static Transwell cell culture inserts was the same as described above. In this case the hEC were cultured on a cell culture insert (PET, 0.4 µm pore size, 12-well system, Costar, Corning Incorporated) coated with Matrigel, at a density of 8×10^4 cells as described previously (Cecchelli et al., 2014; Heymans et al., 2020). For the co-culture, brain pericytes were trypsinized and seeded at a concentration of 2.5×10^4 cells on the bottom of 0.2% gelatin-coated 12-well plates (Costar, Corning Incorporated). During the 7 days of co-culture cells were kept in a CO_2 incubator at 37 ºC, with 5% CO_2.

Static culture conditions in the LOC device

For the static condition, a 20 ml plastic disposable syringe with Luer cone (B. Braun, Melsungen, Germany) containing cell culture medium was placed in a syringe pump (Legato 110, KD Scientific, Holliston, MA, USA) and connected to the inlets/outlets of the LOC device via female Luer locks (Rotilabo, Carl Roth, Karlsruhe, Germany) using plastic tubes (1 mm inner, 3 mm outer diameter, Carl Roth). For the first six days of the dynamic condition and all the seven days of the static condition the syringe was programmed to change medium above the BLEC monolayer every 8 hours at 500 µl/min flow rate. The medium in the lower compartment containing PCs was changed manually daily.

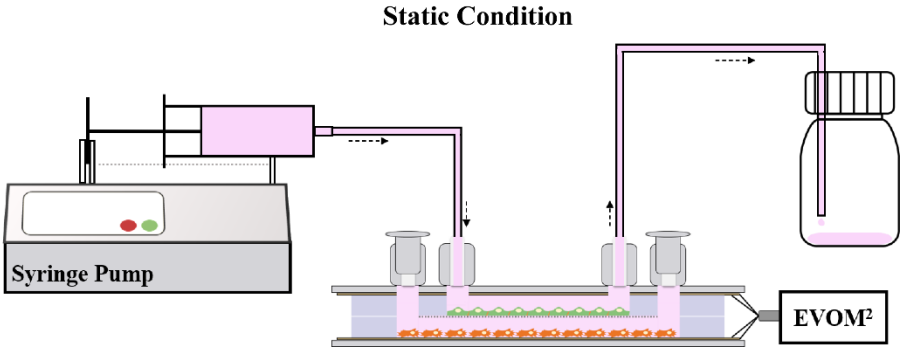

Supplementary Figure S1. Static condition: a syringe containing the cell culture medium was placed in a syringe pump (on the left), which allowed automatic medium change through the top compartment every 8 hours with a fluid flow of 500 µL/min, for 4 minutes. A reservoir was connected to the LOC to collect the discarded medium.

High shear conditions in the LOC device

To increase the shear stress to 1.6 dyne/cm^2 in the LOC device, we elevated the osmolality of the culture medium by the addition of 3.5% dextran (average molecular weight: 60-76 kDa) and at the same time increased the velocity of the fluid flow to 2.5 ml/min. Upon

reaching the 6th day, a constant circulation of culture medium was introduced by a peristaltic pump (Masterflex, Cole-Parmer, USA) at 1ml/min (0.4 dyne/cm^2) or 2.5ml/min (1.6 dyne/cm^2) flow rate for 24 hours. Right after this 24-hour low or high shear we performed barrier integrity studies on the human BBB model, stained BLECs for glycocalyx and TJ proteins, and measured the zeta potential of the cells.

Barrier integrity measurement: permeability

In order to assess the differences between the integrity of BBB models kept in static or dynamic condition we measured the flux of two fluorescent markers of permeability. To assess the barrier integrity small molecular weight marker lucifer yellow (LY, MW: 457 Da) (Cecchelli 2014) and Evans blue dye bound to 1 % bovine serum albumin (EBA, MW: 67.5 kDa) (Walter 2016) were used. For the assay medium in the upper compartments of the LOC devices was replaced with 150 µl of Ringer-Hepes solution (118 mM NaCl, 4.8 mM KCl, 2.5 mM $CaCl_2$, 1.2 mM $MgSO_4$, 5.5 mM D-glucose, 10 mM HEPES, pH 7.4) containing 1 % bovine serum albumin (BSA), 1 % Insulin-Transferrin-Selenium supplement (ITS, Life Technologies), LY (5 µM) and EBA (165 µg/ml dye bound to 1 % BSA). In the bottom compartments, culture medium was changed to 350 µl of Ringer-Hepes solution with 1 % BSA and 1 % ITS. LOCs were incubated for 20, 40 and 60 minutes in a CO_2 incubator at 37 °C on a horizontal shaker (150 rpm/min). Samples were collected from both compartments and fluorescent intensity measured by spectrofluorometer (Horiba Jobin Yvon Fluorolog 3, Kyoto, Japan) at 420 nm excitation and 535 nm emission wavelengths for LY and 582 nm excitation and 662 nm emission wavelengths for EBA.

Concentrations of each marker were determined by plotting them to a calibration curve. First, the clearance (µl) was calculated with the help of the following equation:

$$Cl = \frac{[C]_{ab} \times V_{ab}}{[C]_l}$$

where Cl is the clearance, $[C]_{ab}$ and V_{ab} represent the concentration and volume (µl) of the abluminal (acceptor) compartment, and $[C]_l$ represents the luminal (donor) concentration. Clearance values of the marker molecules were plotted against time (20, 40 and 60 min) and the slope values were used as PS (permeability surface area product). The apparent permeability coefficient (P_{app}) was calculated from the following equation:

$$P_{app} = \frac{PS}{A}$$

where PS was expressed as clearance rate (µl/min) of the BBB models on the membranes, while A was the surface area of the membrane (0.8 cm²).

Immunocytochemistry

To evaluate the morphology of BLECs kept in dynamic or static condition, cells were fixed with ice cold methanol and acetone solution (1:1) for 2 minutes for the junctional staining's and with1% PFA, 15minutes at room temperature for the surface proteins. The membranes with cells were washed twice with phosphate buffered saline (PBS) containing 1% FBS and the non-specific binding sites were blocked with 3 % BSA in

PBS for 1 hour at room temperature. The primary antibodies rabbit anti-β-catenin (#C2206, Sigma, 1:300), rabbit anti-claudin-5 (SAB4502981, Sigma, 1:300), rabbit anti-zonula occluden-1 (61-7300, ThermoFisher Scientific, 1:300), rabbit anti-glut-1 (AB15309, Abcam, 1:100), mouse anti-P-gp (517310, Calbiochem, 1:100), mouse anti-ICAM1 (MA5407, ThermoFisher Scientific, 1:100) mouse anti-VCAM1 (13-1060-82, ThermoFisher Scientific, 1:100) were diluted in 3 % BSA-PBS blocking buffer and incubated with the samples overnight at 4 °C. Next day cells were washed three times with PBS and incubated with secondary antibody anti-rabbit IgG-CY3 (C2306, Sigma, 1:400) or Alexa fluor 488 anti-mouse IgG (A11029, ThermoFisher Scientific, 1:400) and the H33342 dye (1 µg/ml) in PBS for 1 hour at room temperature. The same protocol was used to stain bovine brain PCs with primary antibodies mouse anti-α-SM-actin (A2547, Sigma, 1:200), rabbit anti-NG2 (AB5320, Millipore, Merck, Darmstadt, Germany, 1:200) and rabbit anti-PDGFR-β (ab32570, AbCam, Cambridge, UK, 1:200). Alexa fluor 488 anti-mouse IgG (A11029, ThermoFisher Scientific, 1:400), anti-rabbit IgG-CY3 (C2306, Sigma, 1:400) and H33342 dye (1 µg/ml) were used as a secondary antibodies and staining cell nuclei, respectively. After mounting the samples in Fluoromount-G (Southern Biotech, Birmingham, AL, USA) staining of samples was visualized by a Leica TCS SP5 confocal laser scanning microscope (Leica Microsystems, Wetzlar, Germany).

Total RNA isolation

After 24-hour static or dynamic condition, BLECs were removed from the LOC devices by very fast and gentle trypsinization and RNA was isolated using RNeasy Plus Micro Kit (Qiagen, Hilden, Germany) following the manufacturer's instructions. Integrated gDNA eliminator spin column allows DNA depletion from RNA samples. RNA integrity (supplementary Figure 2) was analyzed using automated capillary electrophoresis (RNA Pico Sensitivity Assay, LabChip GX II Touch HT, Perkin Elmer, Waltham, MA, USA). RNA samples were stored at -80 °C until further analysis.

RNA sequencing and generation of MACE-seq libraries

Samples with 100 ng of purified RNA were used for library preparation. RNA was fragmented using GenXPro Fragmentation Buffer. Synthesis of cDNA was performed by reverse transcription using barcoded oligo(dT) primers containing *TrueQuant* unique molecular identifiers, followed by template switching. Library amplification was done using polymerase chain reaction (PCR), purified by solid phase reversible immobilization beads (Agencourt AMPure XP, Beckman Coulter, Brea, CA, USA) and subsequent sequencing was performed using a NextSeq platform (Illumina Inc., San Diego, CA, USA).

Zeta potential measurements

The zeta potential was measured at 25 °C, from a minimum of 6 measurements (maximum 100 runs for each) with an applied voltage of 20 V. The disposable zeta potential cuvettes, equipped with gold plated beryllium/copper electrodes (DTS1070, Malvern, UK), were activated before the initial measurements with 100 % methanol and

rinsed with distilled water twice, then calibrated with a zeta standard solution as described in the manufacturer's protocol. After 24-hour dynamic and static condition BLECs were quickly and gently trypsinized, centrifuged and 10^5 cells were pipetted in 900 μL PBS with Ca^{2+} and Mg^{2+} into the cuvettes and zeta potential was measured. The Zetasizer Software v.7.12. calculated the zeta potential values (in mV) using the Smoluchowski equation.

The co-culture of BLECs with brain pericytes was performed on the cell culture inserts as described above and was compared with the monocultures of the hECs. The zeta measurement and the fluorescently labeled wheat germ agglutinin staining labeling of sialic acid and N-acetyl-D-glucosamine residues within the glycocalyx were done as described for cells in the LOC device.

Results

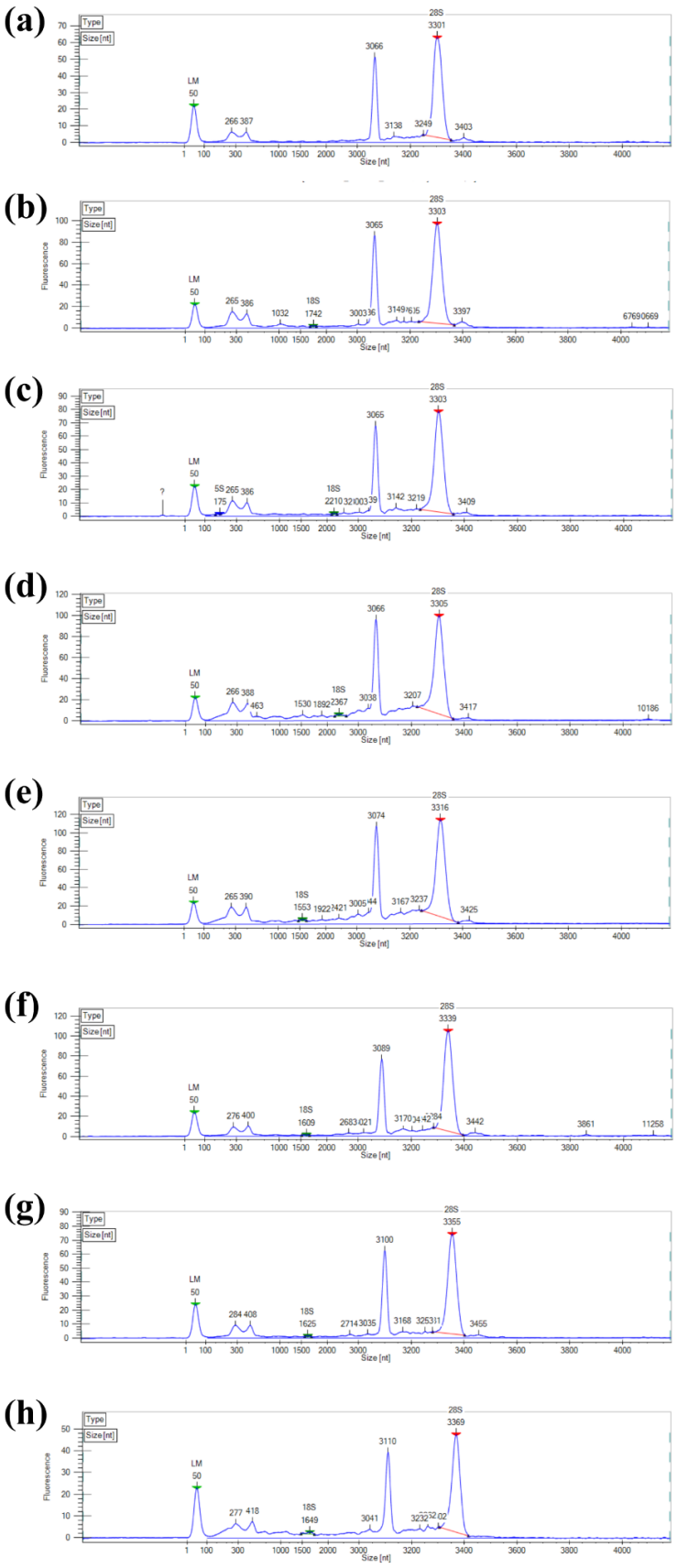

Supplementary Figure S2. Quality control for RNA for each sequenced sample. (a)-(e) Dynamic condition samples. (f)-(h) Static condition samples.

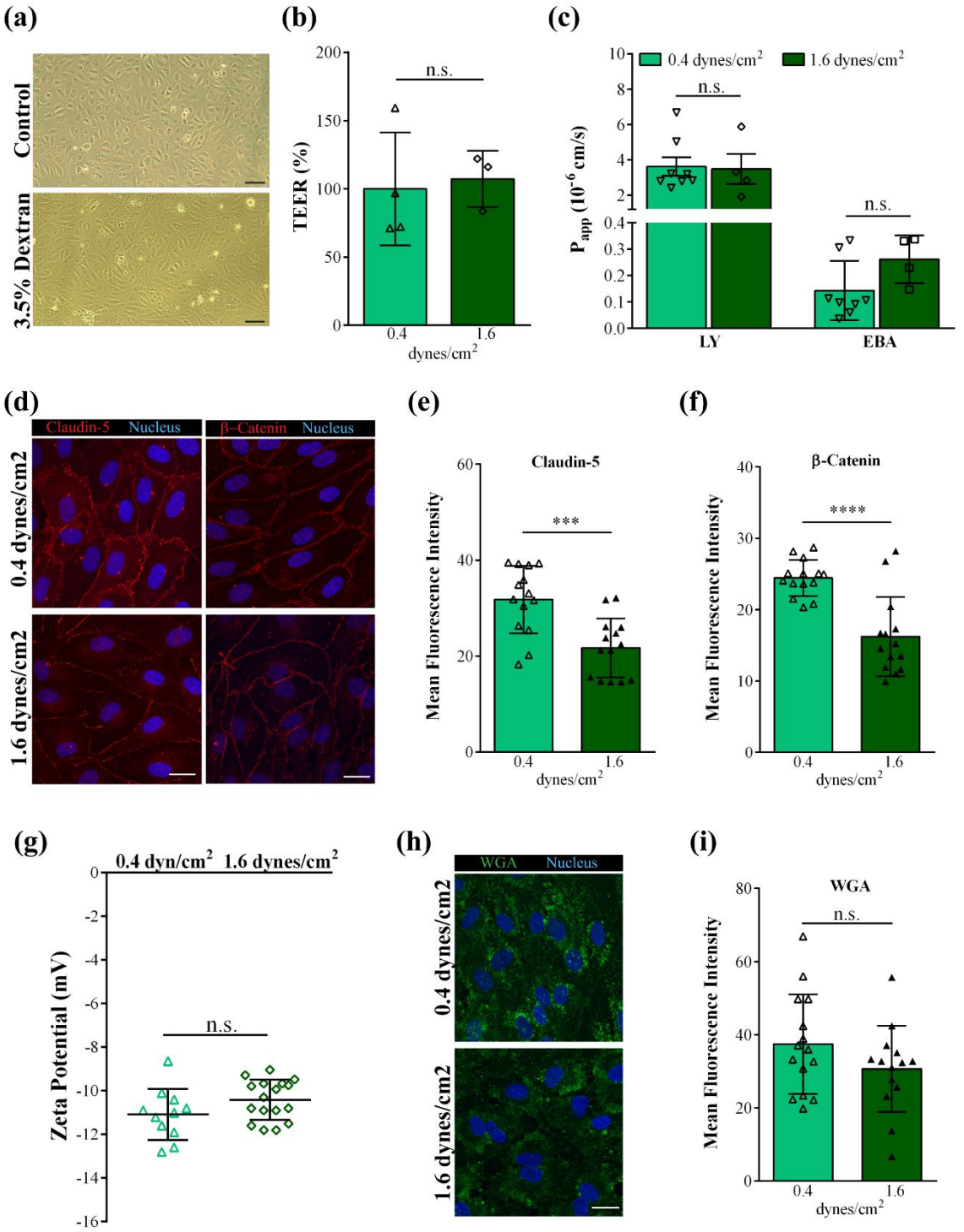

Figure S3. Comparison of 0.4 dyne/cm^2 and 1.6 dyne/cm^2 shear stress on the human BBB model. Cells were exposed to fluid flow for 24-hours before the evaluation of barrier integrity and morphology. (a) Phase contrast images of brain endothelial cells with and without 3.5% dextran. Scale bar: 100 µm. (b) TEER results expressed as % of the 0.4 dyne/cm^2 group (n=3-4). (c) Apparent permeability coefficient (P_{app}) of the human BBB model for Lucifer yellow (LY) and Evans blue labeled albumin (EBA) marker molecules (n=4-8). (d-f) Immunostaining for claudin-5 and β-catenin junctional proteins and fluorescent intensity analysis of the images (n= 14; ***p<0.001, ****p<0.0001 compared to 0.4 dyne/cm^2 shear stress group.) (g) Zeta potential measured by laser Doppler velocimetry (n=11-17). (h-i) Staining of endothelial surface glycocalyx on brain endothelial cells with fluorescently labeled wheat germ agglutinin (WGA) lectin, binding to the sialic acid residues. Fluorescent intensity of the images shows the thickness and density of the glycocalyx components. (n= 14) Scale bars for all fluorescent images: 20 µm. All values are presented as means ± SD; statistical analysis unpaired t-test. n.s., not significant.

We evaluated the effects of a four-times higher, 1.6 dynes/cm^2 shear stress, that can be considered as physiological, on the human BBB model (Fig. S3). We achieved this by increasing both the velocity of the fluid flow (2.5 ml/min) and the osmolality of the medium by adding 3.5% dextran. BLECs tolerated well the presence of dextran, no change in cell morphology was visible (Figure S3 (a)). We found no difference between the TEER values of the 0.4 and 1.6 dynes/cm^2 shear groups (Figure S3 (b)). In permeability experiments using LY and EBA markers an increased barrier integrity was found for both high and low shear conditions as compared to the static culture (Figure 1 in the main text). No difference was observed between the P_{app} values of the 0.4 vs 1.6 dynes/cm^2 groups (Figure S3 (c)) indicating, that the higher shear, at least in this range, did not strengthen the barrier more than the 0.4 dynes/cm^2 condition.

Immunostaining for junctional markers was performed for BLECs in dynamic conditions and staining intensity was evaluated by the ImageJ software. In the 1.6 dynes/cm^2 shear group we found a decreased immunostaining intensity for the claudin-5 in comparison with the 0.4 dynes/cm^2 conditions (Figure S3 (d-e)). Similar observation was made regarding the β-catenin expression, where a decreased fluorescence intensity was measured in the higher shear group (Figure S3 (d) and (f)). We analyzed the staining for the sialic acid residuess of the surface glycocalyx with WGA lectin and we saw no difference between the lower and the higher shear stress groups (Figure S3 (h and i)). Moreover, the zeta potential in the two dynamic groups was also not different from each other (Figure S3 (g)). Based on these observations, we can conclude that the 1.6 dynes/cm^2 shear condition was well-tolerated by the BLECs, and it was similarly beneficial to the barrier integrity elevation and glycocalyx expression as the 0.4 dynes/cm^2 shear condition. In our experimental setup this lower shear stress provided sufficient dynamic condition for the BLEC/bovine pericyte model to observe improved barrier integrity and the expression of important BBB genes and characteristics.

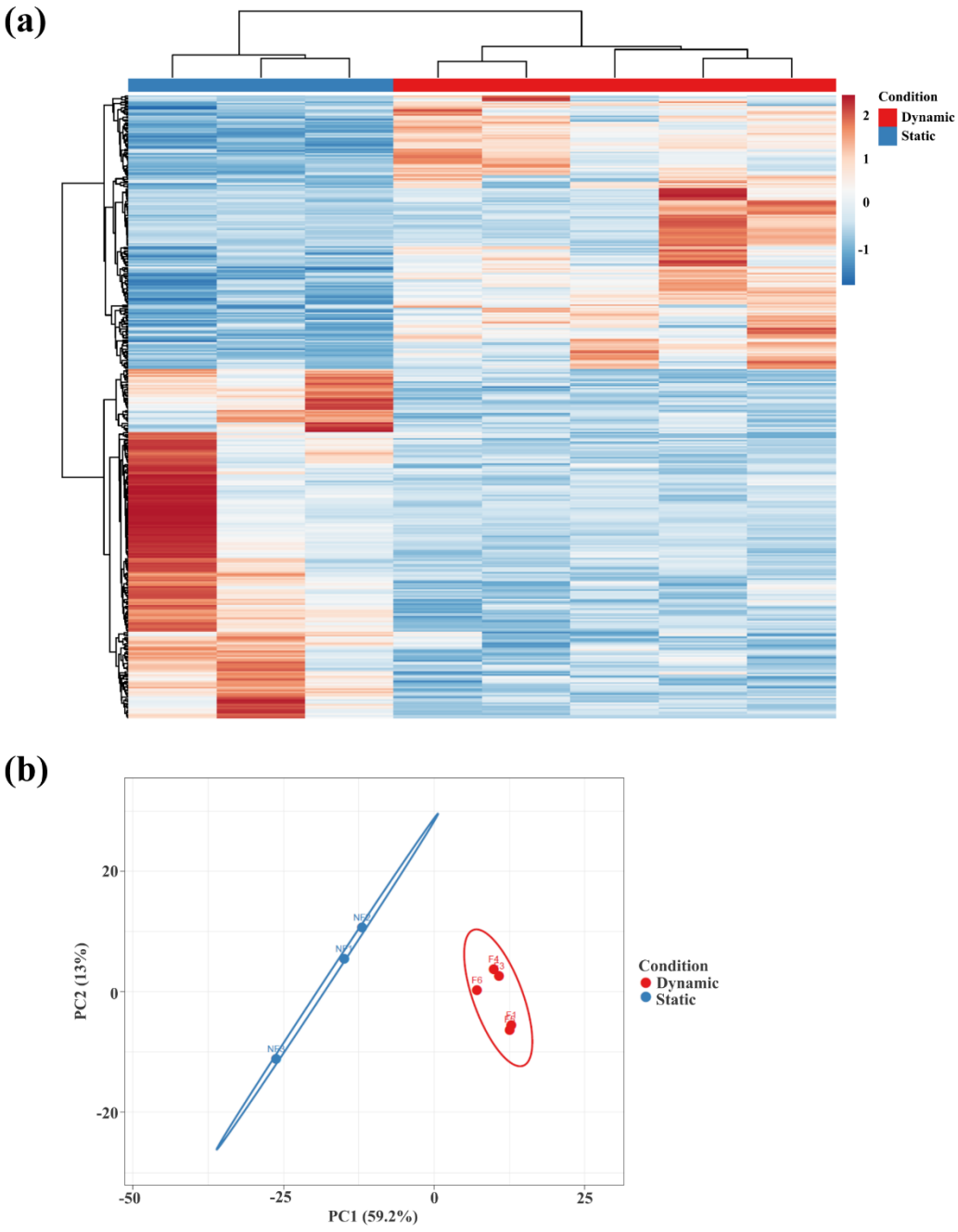

Supplementary Figure S4. General transcriptomic profile. (a) Heat map of all differentially expressed genes. Data input consisted of the normalized expression in flow condition(dynamic) compared with no flow condition (static). Unit variance scaling is applied to rows. (b) Principal component (PC) analysis and hierarchical clustering were used to assess relatedness between samples.

Supplementary Table S1. Top 50 differentially expressed genes in the human BBB model in dynamic condition. Colors highlight the genes discussed in the results section of the study. Red color labels gene upregulation and blue color shows gene downregulation.

Gene symbol	Description	P-value	Log2FC
TSPAN15	tetraspanin 15	1,43E-34	1,33
CYP1A1	cytochrome P450 family 1 subfamily A member 1	1,42E-25	2,70
PLVAP	plasmalemma vesicle associated protein	4,13E-23	1,95
MMP10	matrix metallopeptidase 10	5,29E-23	2,16
TGFBI	transforming growth factor beta induced	6,51E-19	1,86
PMEPA1	prostate transmembrane protein, androgen induced 1	1,62E-18	1,51
SNAI1	snail family transcriptional repressor 1	3,84E-18	1,49
ANPEP	alanyl aminopeptidase, membrane	7,61E-14	1,11
ALDH1A2	aldehyde dehydrogenase 1 family member A2	2,98E-13	-1,93
GJA5	gap junction protein alpha 5	1,61E-12	2,69
SPSB1	splA/ryanodine receptor domain and SOCS box containing 1	1,67E-12	1,24
MEF2C	myocyte enhancer factor 2C	2,19E-12	-1,05
RASD1	ras related dexamethasone induced 1	1,08E-11	2,05
CCL2	C-C motif chemokine ligand 2	1,27E-11	1,61
ICAM1	intercellular adhesion molecule 1	1,49E-11	1,38
KRT19	keratin 19	6,39E-11	-1,75
HTRA1	HtrA serine peptidase 1	2,01E-10	1,08
NR5A2	nuclear receptor subfamily 5 group A member 2	6,40E-10	-1,47
ENG	endoglin	9,97E-10	1,02
CRLF1	cytokine receptor like factor 1	1,16E-09	2,64
PDLIM1	PDZ and LIM domain 1	1,71E-09	-1,15
AKR1C3	aldo-keto reductase family 1 member C3	4,97E-09	1,21
CXCL6	C-X-C motif chemokine ligand 6	7,74E-09	-2,15
SERINC2	serine incorporator 2	8,76E-09	1,17
TAGLN	transgelin	1,88E-08	1,94
NR4A1	nuclear receptor subfamily 4 group A member 1	4,41E-08	-3,57
PSAT1	phosphoserine aminotransferase 1	4,73E-08	-1,04
MAN1C1	mannosidase alpha class 1C member 1	5,51E-08	-2,45
LYVE1	lymphatic vessel endothelial hyaluronan receptor 1	5,83E-08	-3,69
TMCC3	transmembrane and coiled-coil domain family 3	7,08E-08	-1,22
LAPTM5	lysosomal protein transmembrane 5	1,23E-07	1,25
FAM129A	family with sequence similarity 129 member A	2,00E-07	-2,66
DIRAS3	DIRAS family GTPase 3	2,17E-07	-1,76
SLC2A6	solute carrier family 2 member 6	2,32E-07	1,11
NQO1	NAD(P)H quinone dehydrogenase 1	2,32E-07	1,13
ADORA2A	adenosine A2a receptor	2,61E-07	-1,31
AC078850.1	NA	2,75E-07	-1,90
COL4A1	collagen type IV alpha 1 chain	6,38E-07	1,12
PAPPA	pappalysin 1	9,14E-07	2,56
EXOC3L1	exocyst complex component 3 like 1	1,01E-06	2,81
OSGIN1	oxidative stress induced growth inhibitor 1	1,25E-06	1,43
CHST1	carbohydrate sulfotransferase 1	1,67E-06	1,22
LRRC8B	leucine rich repeat containing 8 VRAC subunit B	1,89E-06	-1,07
VCAN	versican	2,38E-06	3,89
SLC7A2	solute carrier family 7 member 2	2,65E-06	1,24
F2RL3	F2R like thrombin or trypsin receptor 3	4,09E-06	2,17
TNFSF15	TNF superfamily member 15	5,87E-06	1,22
DUSP5	dual specificity phosphatase 5	5,97E-06	-1,37
NAB2	NGFI-A binding protein 2	6,92E-06	-1,13
PANX2	pannexin 2	7,59E-06	1,37

Supplementary Table S2. Top 50 upregulated genes in the human BBB model in dynamic condition. Red color highlight the genes discussed in the results section of the study.

Gene symbol	Description	P-value	Log2FC
TSPAN15	tetraspanin 15	1,43E-34	1,33
CYP1A1	cytochrome P450 family 1 subfamily A member 1	1,42E-25	2,70
PLVAP	plasmalemma vesicle associated protein	4,13E-23	1,95
MMP10	matrix metallopeptidase 10	5,29E-23	2,16
TGFBI	transforming growth factor beta induced	6,51E-19	1,86
PMEPA1	prostate transmembrane protein, androgen induced 1	1,62E-18	1,51
SNAI1	snail family transcriptional repressor 1	3,84E-18	1,49
ANPEP	alanyl aminopeptidase, membrane	7,61E-14	1,11
GJA5	gap junction protein alpha 5	1,61E-12	2,69
SPSB1	splA/ryanodine receptor domain and SOCS box containing 1	1,67E-12	1,24
RASD1	ras related dexamethasone induced 1	1,08E-11	2,05
CCL2	C-C motif chemokine ligand 2	1,27E-11	1,61
ICAM1	intercellular adhesion molecule 1	1,49E-11	1,38
HTRA1	HtrA serine peptidase 1	2,01E-10	1,08
ENG	endoglin	9,97E-10	1,02
CRLF1	cytokine receptor like factor 1	1,16E-09	2,64
AKR1C3	aldo-keto reductase family 1 member C3	4,97E-09	1,21
SERINC2	serine incorporator 2	8,76E-09	1,17
TAGLN	transgelin	1,88E-08	1,94
LAPTM5	lysosomal protein transmembrane 5	1,23E-07	1,25
SLC2A6	solute carrier family 2 member 6	2,32E-07	1,11
NQO1	NAD(P)H quinone dehydrogenase 1	2,32E-07	1,13
COL4A1	collagen type IV alpha 1 chain	6,38E-07	1,12
PAPPA	pappalysin 1	9,14E-07	2,56
EXOC3L1	exocyst complex component 3 like 1	1,01E-06	2,81
OSGIN1	oxidative stress induced growth inhibitor 1	1,25E-06	1,43
CHST1	carbohydrate sulfotransferase 1	1,67E-06	1,22
VCAN	versican	2,38E-06	3,89
SLC7A2	solute carrier family 7 member 2	2,65E-06	1,24
F2RL3	F2R like thrombin or trypsin receptor 3	4,09E-06	2,17
TNFSF15	TNF superfamily member 15	5,87E-06	1,22
PANX2	pannexin 2	7,59E-06	1,37
MYLK2	myosin light chain kinase 2	1,27E-05	2,33
SERPINE2	serpin family E member 2	1,42E-05	1,41
RASA4	RAS p21 protein activator 4	2,40E-05	1,44
DYRK1B	dual specificity tyrosine phosphorylation regulated kinase 1B	3,57E-05	1,05
SERPINE1	serpin family E member 1	3,66E-05	1,17
RASA4B	RAS p21 protein activator 4B	4,10E-05	1,51
RFX2	regulatory factor X2	4,31E-05	1,13
LFNG	LFNG O-fucosylpeptide 3-beta-N-acetylglucosaminyltransferase	4,44E-05	1,02
LIPG	lipase G, endothelial type	6,65E-05	2,26
ITGA11	integrin subunit alpha 11	8,03E-05	1,33
ZNF704	zinc finger protein 704	0,000119	1,01
SEMA3G	semaphorin 3G	0,000127	2,65
SLC25A34-AS1	SLC25A34 and TMEM82 antisense RNA 1	0,000166	1,22
ZNF365	zinc finger protein 365	0,000186	1,76
SDC2	syndecan 2	0,000205	1,22
EPS8L1	EPS8 like 1	0,000228	1,08
PCDH9	protocadherin 9	0,000243	1,23
MYLK	myosin light chain kinase	0,000278	1,04

Supplementary Table S3. Top 50 downregulated genes in the human BBB model in dynamic condition. Blue color highlight the genes discussed in the results section of the study.

Gene symbol	Description	P-value	Log2FC
ALDH1A2	aldehyde dehydrogenase 1 family member A2	2,98E-13	-1,93
MEF2C	myocyte enhancer factor 2C	2,19E-12	-1,05
KRT19	keratin 19	6,39E-11	-1,75
NR5A2	nuclear receptor subfamily 5 group A member 2	6,40E-10	-1,47
PDLIM1	PDZ and LIM domain 1	1,71E-09	-1,15
CXCL6	C-X-C motif chemokine ligand 6	7,74E-09	-2,15
PSAT1	phosphoserine aminotransferase 1	4,73E-08	-1,04
MAN1C1	mannosidase alpha class 1C member 1	5,51E-08	-2,45
TMCC3	transmembrane and coiled-coil domain family 3	7,08E-08	-1,22
FAM129A	family with sequence similarity 129 member A	2,00E-07	-2,66
DIRAS3	DIRAS family GTPase 3	2,17E-07	-1,76
ADORA2A	adenosine A2a receptor	2,61E-07	-1,31
AC078850.1	NA	2,75E-07	-1,90
LRRC8B	leucine rich repeat containing 8 VRAC subunit B	1,89E-06	-1,07
DUSP5	dual specificity phosphatase 5	5,97E-06	-1,37
NAB2	NGFI-A binding protein 2	6,92E-06	-1,13
KCNAB1	potassium voltage-gated channel subfamily A member regulatory beta subunit 1	8,14E-06	-1,21
DPP4	dipeptidyl peptidase 4	1,02E-05	-1,72
AGFG2	ArfGAP with FG repeats 2	1,39E-05	-1,06
CLDN7	claudin 7	1,65E-05	-1,32
UCP2	uncoupling protein 2	1,70E-05	-1,38
UBXN2B	UBX domain protein 2B	2,06E-05	-1,04
CCL14	C-C motif chemokine ligand 14	3,60E-05	-2,18
VSIR	V-set immunoregulatory receptor	6,96E-05	-1,24
METTL7A	methyltransferase like 7A	9,20E-05	-1,04
WDR27	WD repeat domain 27	0,000103	-1,39
GPRC5A	G protein-coupled receptor class C group 5 member A	0,00011	-1,02
RHPN1	rhophilin Rho GTPase binding protein 1	0,000189	-1,14
OAS3	2'-5'-oligoadenylate synthetase 3	0,000214	-1,13
JMJD1C-AS1	JMJD1C antisense RNA 1	0,000245	-2,58
ATP2A3	ATPase sarcoplasmic/endoplasmic reticulum Ca2+ transporting 3	0,000259	-2,24
AC007998.3	NA	0,000283	-2,07
MME	membrane metalloendopeptidase	0,000289	-1,14
ELMOD1	ELMO domain containing 1	0,000334	-2,28
IL27RA	interleukin 27 receptor subunit alpha	0,00035	-1,15
SMPDL3B	sphingomyelin phosphodiesterase acid like 3B	0,000365	-1,75
CDKN2A	cyclin dependent kinase inhibitor 2A	0,000385	-1,10
SLC22A23	solute carrier family 22 member 23	0,000414	-1,33
AC012653.2	NA	0,000434	-1,32
G0S2	G0/G1 switch 2	0,000448	-1,90
KHK	ketohexokinase	0,000478	-1,53
TCF15	transcription factor 15	0,000494	-1,41
N4BP2L1	NEDD4 binding protein 2 like 1	0,000497	-1,75
AQP3	aquaporin 3 (Gill blood group)	0,00055	-1,22
RASSF4	Ras association domain family member 4	0,00063	-1,25
RARRES1	retinoic acid receptor responder 1	0,000649	-1,82
KIAA0040	KIAA0040	0,000688	-1,52
ENPP2	ectonucleotide pyrophosphatase/phosphodiesterase 2	0,000695	-2,51
AK5	adenylate kinase 5	0,000796	-1,02
MPZL2	myelin protein zero like 2	0,000883	-1,23

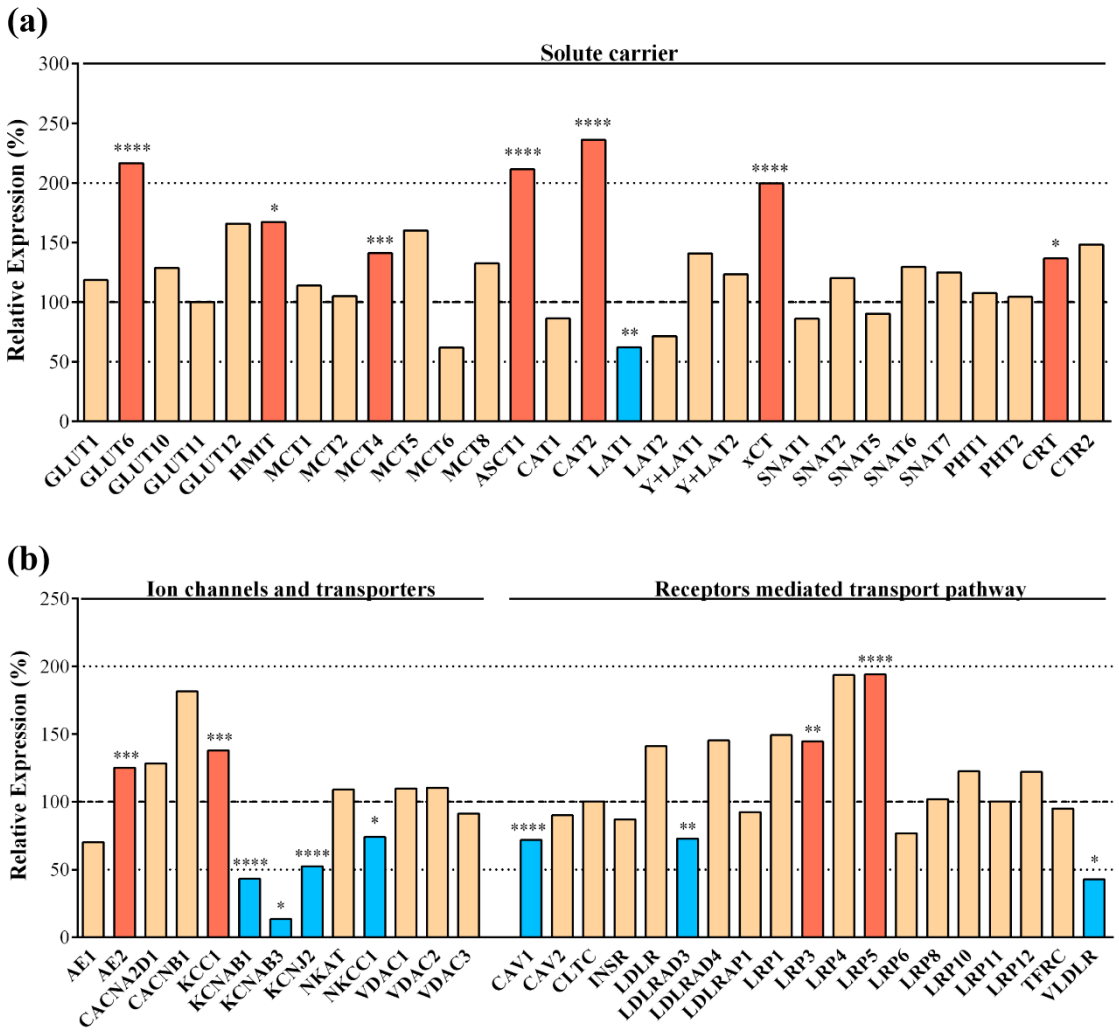

Supplementary Figure S5. Transcriptomic gene expression profile of (a) solute carrier genes and (b) ion channel and transporter, and receptor mediated transport pathway-related genes. Expression is shown as the relative expression (%) of the genes present in human endothelial cells co-cultured with brain pericytes in dynamic condition as compared to static condition. Genes with a p-value < 0.05 and less than 50% or more than 200% gene expression levels were considered to be differentially expressed. Red color labels upregulation and statistically significant expression changes, blue color shows downregulation and statistically significant expression change, cream color indicates no change in the gene expression (*p<0.05, **p<0.01, ***p<0.001, ****p<0.0001).

SLCs are abundantly expressed at the BBB (Daneman et al., 2010; Campos-Bedolla et al., 2014; Veszelka et al., 2018). Glucose transporters, like SLC2A1 (GLUT1), SLC2A10 (GLUT10), SLC2A11 (GLUT11) and SLC2A12 (GLUT12) were expressed with an unchanged level, while SLC2A6 (GLUT6) and SLC2A13 (GLUT13/HMIT) were significantly overexpressed after flow (Figure S5(a)). Genes for six monocarboxylate transporters, involved in the transport of lactate, pyruvate, ketone bodies and thyroid hormones, were expressed in BLECs. No change was seen in their expression level after flow, except for SLC16A4 (MCT4) which was significantly elevated (Figure S5(a)). From the large family of amino acid transporters most genes were present at an unchanged level. We found three genes in this group which were upregulated by flow, the sodium-dependent neutral amino acid transporter SLC1A4 (ASCT1), the cationic amino acid

transporter SLC7A2 (CAT2) and the chloride dependent cystine-glutamate antiporter SLC7A11 (xCT), and only one gene, SLC7A5 (LAT1), which was downregulated (Figure 5(a)). The expression levels of the peptide transporters SLC15A4 (PHT1) and SLC15A3 (PHT2) were not changed by fluid flow (Figure S5(a)). The creatine transporter SLC6A8 (CRT) was significantly upregulated in dynamic condition, while the copper transporter SLC31A2 (CTR2) was not.

Several ion transporters, pumps and channels are expressed at the BBB (Sweeney et al., 2019), that we could confirm in our study (Figure S5(b)). We found no change by flow in the gene expression of the anion exchanger-1 (SLC4A1/AE1), preproteins for voltage-gated Ca^{2+} channel subunits (CACNA2D1 and CACNB1), the Na^{+}/K^{+} ATPase (ATP1A1/NKAT), and voltage dependent anion channels (VDAC1-3). Two genes were upregulated after the flow condition, the HCO_3^{-}-Cl^{-} exchanger SLC4A2 (AE2) and the K^{+}- Cl^{-} cotransporter SLC12A4 (KCC1) (Figure S5(b)). Flow condition downregulated the expression of the voltage-gated K^{+} channel K_v1 subunits (KCNAB1 and KCNAB3) and the $K_{ir}2.1$ inward-rectifier K^{+} channel (KCNJ2), and the Na^{+}-K^{+}-Cl^{-} cotransporter-1 (SLC12A2/NKCC1).

The penetration of peptides, proteins and lipoproteins through the BBB are controlled by the receptor mediated transporters (Sweeney et al., 2019). We detected the presence of many important BBB receptor genes on the human BBB model (Figure S5(b)). Most of these were not changed by flow, including insulin receptor (INSR), members of the low density lipoprotein receptor family (LDLR, LDLRAD4, LDLRAP1), members of the low density lipoprotein receptor related protein family (LRP1, LRP4, LRP6, LRP8, LRP10, LRP11, LRP12) and transferrin receptor (TFRC). Dynamic condition increased the expression of two receptor genes, LRP3 and LRP5 and decreased the level of LDLRAD3 and very low density lipoprotein receptor (VLDLR). Caveolins regulate endocytosis, transcytosis and signalling in lipid-base domains; the expression level of caveolin-1 (CAV1) gene was decreased by flow, while the expression of CAV2 and clathrin (CLTC) was not changed (Figure S5(b)).

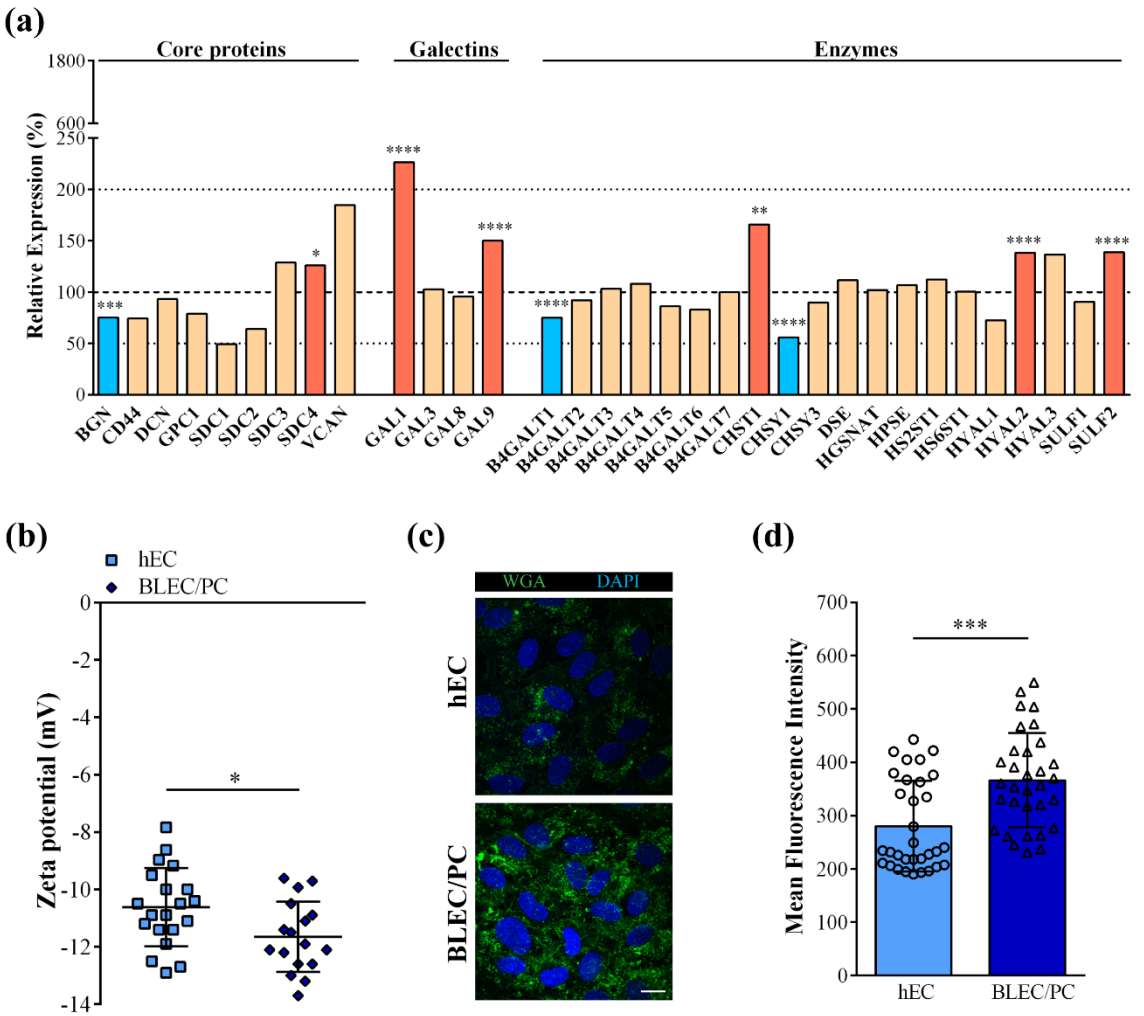

Supplementary Figure S6. Endothelial surface glycocalyx (ESG) of the human BBB model on cell culture inserts (BLEC/PC). (a) Transcriptomic gene expression profile of ESG-related genes. Expression is shown as the relative expression (%) of the genes present in human endothelial cells co-cultured with brain pericytes (BLEC/PC) in static condition as compared to solo culture (hEC) (MACE-seq dataset: GSE144474, Heymans et al., 2020). Testing for differential gene expression was performed using the DESeq2 R/Bioconductor package (Love et al., 2014). Genes with a p-value < 0.05 and less than 50% or more than 200% gene expression levels were considered to be differentially expressed. Red color labels upregulation and statistically significant expression changes, blue color shows downregulation and statistically significant expression change, cream color indicates no change in the gene expression (*p<0.05, **p<0.01, ***p<0.001, ****p<0.0001). (b) Zeta potential measured by laser Doppler velocimetry (means ± SD, n=17-23, unpaired t-test, *p<0.05 compared to monoculture). (c) and (d): Staining of ESG on brain endothelial cells with fluorescently labeled wheat germ agglutinin (WGA) lectin. WGA binds to the sialic acid residues therefore the fluorescent intensity of the images shows the thickness and density of the glycocalyx components. Scale bar: 20 µm. Image analysis values are presented as means ± SD, n=32; unpaired t-test, ***p<0.001 compared to the human endothelial cells (hEC).

References

Campos-Bedolla P, Walter FR, Veszelka S, et al. Role of the blood-brain barrier in the nutrition of the central nervous system. *Arch Med Res* 2014;45(8):610-638.

Cecchelli R, Aday S, Sevin E, et al. A stable and reproducible human blood-brain barrier model derived from hematopoietic stem cells. *PLoS One* 2014;9(6):e99733.

Coecke S, Balls M, Bowe G, et al. Guidance on good cell culture practice. a report of the second ECVAM task force on good cell culture practice. *Altern Lab Anim*. 2005 Jun;33(3):261-87.

Daneman R, Zhou L, Agalliu D, et al. The mouse blood-brain barrier transcriptome: a new resource for understanding the development and function of brain endothelial cells. *PLoS One* 2010; 5(10):e13741.

Heymans M, Figueiredo R, Dehouck L, et al. Contribution of brain pericytes in blood-brain barrier formation and maintenance: a transcriptomic study of cocultured human endothelial cells derived from hematopoietic stem cells. *Fluids Barriers CNS* 2020;17(1):48.

Love MI, Huber W and Anders S. Moderated estimation of fold change and dispersion for RNA-seq data with DESeq2. *Genome Biol* 2014;15(12):550.

Pedroso DC, Tellechea A, Moura L, Fidalgo-Carvalho I, Duarte J, Carvalho E, Ferreira L. Improved survival, vascular differentiation and wound healing potential of stem cells co-cultured with endothelial cells. *PLoS One*. 2011 Jan 24;6(1):e16114.

Sweeney MD, Zhao Z, Montagne A, et al. Blood-Brain Barrier: From Physiology to Disease and Back. *Physiol Rev* 2019;99(1):21-78

Veszelka S, Tóth A, Walter FR, et al. Comparison of a Rat Primary Cell-Based Blood-Brain Barrier Model with Epithelial and Brain Endothelial Cell Lines: Gene Expression and Drug Transport. *Front Mol Neurosci* 2018;11:166.